6810 *Macromolecules* **1997,** *30,* 6810−6813

Ordered Diblock Copolymer Films on Random Copolymer Brushes

P. Mansky and T. P. Russell*

Polymer Science and Engineering Department, Silvio O. Conte Center for Polymer Research, University of Massachusetts, Amherst, Massachusetts 01003

C. J. Hawker

IBM Almaden Research Center, 650 Harry Road, San Jose, California 95120-6099

M. Pitsikalis and J. Mays

Department of Chemistry, University of Alabama at Birmingham, Birmingham, Alabama 35294-1240

Received May 13, 1997; Revised Manuscript Received August 18, 1997[⊗]

ABSTRACT: Optical microscopy, neutron reflectivity, and small angle neutron scattering studies were used to investigate the structure of thin films of symmetric diblock copolymers of P(dS-*b*-MMA) as the interactions between the copolymer and the substrate were changed in a systematic manner. In cases where there was a strong preferential segregation of one of the components to the substrate, the lamellar microdomains were oriented parallel to the film surface. However, on a nearly neutral substrate, a mixed morphology was found where the lamellae adjacent to the free surface are oriented parallel to the plane of the film, while the lamellae adjacent to the substrate are oriented normal to the plane of the film.

The physics of amorphous, flexible diblock copolymer melts is well understood. In the bulk, the morphologies and phase transitions observed result from a balance between the energy associated with interactions between unlike segments at the microdomain interfaces and the entropy associated with chain stretching and the restriction of the junction points to the interfaces.[1−3] In the case of thin films, however, two additional factors come into play: the interactions of the blocks with the film surfaces (wetting effects) and the relationship between the film thickness and the natural period of the bulk microphase-separated structure (commensurability effects).

Commensurability effects in thin films of symmetric diblock copolymers have been extensively studied, in the case of strong wetting of each interface by one or the other block.[4−8] The strong surface interactions force the lamellae to orient parallel to the plane of the film. For unconfined or free films, where there is at least one interface with a vacuum, the film thickness is quantized in terms of the bulk period L_0. If the initial film thickness is not commensurate with this constraint, then an incomplete top layer forms, composed of "islands" or "holes" of height L_0.[4−6] If the films are confined between parallel impenetrable walls, having strong interactions with either block, the frustration imposed by an incommensurate film thickness cannot be relieved by island or hole formation. Instead, the fundamental repeat period is altered[7,8] and the copolymer chains stretch or compress in response to the constraint.

It has recently been shown that the interfacial energies of a given pair of polymers (denoted A and B) with a solid surface can be precisely controlled by end-grafting a layer of A−B random copolymer chains, denoted P(A-*r*-B), to the surface, where the fraction *f* of A monomers in the brush can be varied through synthesis.[9−12] As *f* is varied from 0 to 1, the system passes from strong wetting of the brush by B to strong wetting by A in a continuous fashion, including the case of *neutrality* (nonpreferential wetting). This was demonstrated with A = styrene (S) and B = methyl methacrylate (MMA). It was found that a P(S-*r*-MMA) brush surface has equal interfacial energies with PS and with PMMA when $f = 0.57$.

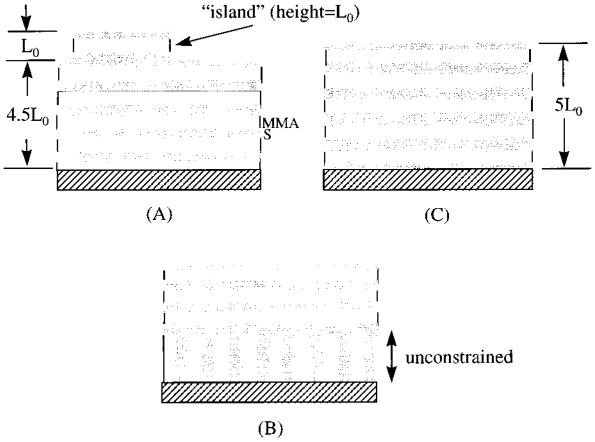

Figure 1. Schematic of the three types of film structures described in this report. The average film thickness is $5L_0$ in all three cases. The preferred film thicknesses are $t = (n + 1/2)L_0$ and $t = nL_0$ for types A and C, respectively, and excess material forms an incomplete top layer. On a neutral surface (type B), the lamellae next to the brush are oriented normal to the substrate. The height of this layer is unconstrained, and the free surface remains flat for all thicknesses. The depiction of the interface between the two regions in (B) is purely schematic.

Here, the effect of tunable surface interactions on the structure of thin films of microphase-separated, symmetric, diblock copolymers is discussed. Three distinct morphologies are found as *f* is varied. For $f < 0.5$ and $f > 0.65$, the lamellae orient *parallel* to the plane of the substrate in the usual manner. Incommensurability is relieved by the formation of islands or holes on the surface. The preferred thicknesses differ in these two cases, however, due to the different boundary conditions

---

[⊗] Abstract published in *Advance ACS Abstracts,* October 1, 1997.

S0024-9297(97)00675-X CCC: $14.00

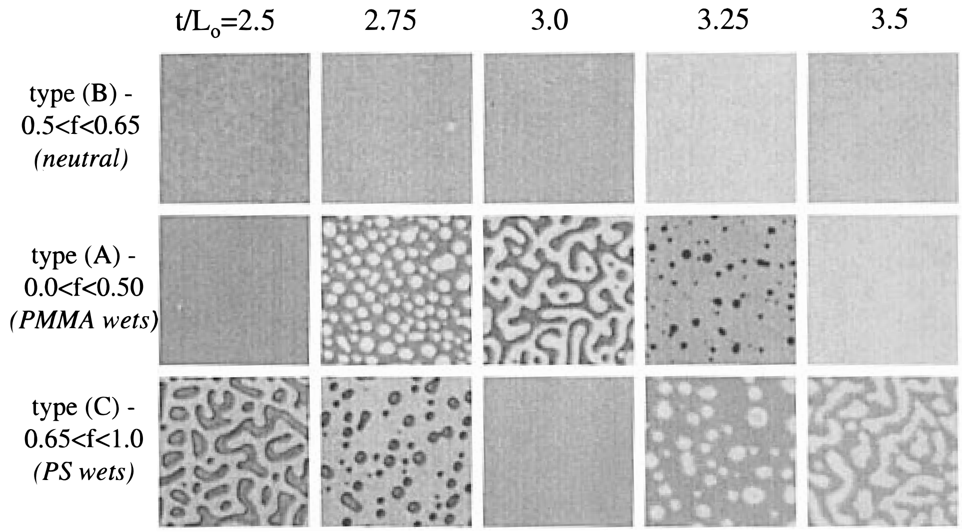

Figure 2. Reflection optical micrographs of P(S-*b*-MMA) films on Si substrates coated with P(S-*r*-MMA) brushes. The film thicknesses in each column are identical, and only the composition of the anchored brush is changed. The film thickness increases from ~2.5L_0 to ~3.5L_0 from left to right.

at the substrate. For $f > 0.65$, PS wets both the air and substrate interfaces ("symmetric wetting") and the preferred thicknesses are $t = nL_0$, where n is an integer. For $f < 0.5$, PMMA wets the brush ("antisymmetric wetting") and $t = (n + 1/2)L_0$ are the preferred thicknesses. For $0.5 < f < 0.65$, when the brush surface is nearly neutral, a "mixed" morphology is found, where the lamellae adjacent to the brush/substrate orient *perpendicular* to the film plane, while the lamellae adjacent to the free surface are still oriented parallel to the surface of the film. These three structures will be referred to as types A, B, and C, as shown schematically in Figure 1. PS wets the vacuum interface in all three cases since its surface tension is lower than that of PMMA.

P(S-*r*-MMA) random copolymer brushes ($M_n = 10\,000$ g, $M_w/M_n = 1.3-1.8$), ~50 Å thick, were end-grafted onto the native oxide layer of silicon wafers as described previously.[11] The P(dS-*b*-MMA) diblock copolymer used in this study was synthesized anionically, with $M_n = 37\,000$, $M_w/M_n = 1.35$, and a dPS volume fraction of 0.53. Block copolymer films of various thicknesses were spin coated from toluene solutions onto silicon substrates, previously modified with the P(S-*r*-MMA) brushes. The samples were annealed in vacuum at 170 °C for 3 days.

The surface topographies of P(dS-*b*-MMA) films on substrates modified with the P(S-*r*-MMA) brushes are shown in the reflection optical micrographs in Figure 2, as a function of the film thickness and the composition of the brush. Three distinct classes were evident and are exemplified by the data in Figure 2. Samples on brushes with $f < 0.5$ (A) and $f \geq 0.65$ (C) showed island and hole formation on the surface. The preferred film thicknesses in case A are $(n + 1/2)L_0$ and in case C are nL_0. These constraints differ by $L_0/2$, and consequently, the fraction of the surface covered by the incomplete top layer differs by 50% for case A and C samples of identical thicknesses prior to annealing. In addition, the interference colors are distinctly different and characteristic of the different thickness constraints placed on the samples. However, samples in case B, where $0.5 < f < 0.65$, had flat surfaces *regardless* of the film thickness and did not exhibit any island or hole formation. (This is strictly true for films more than ~2L_0 thick. Thinner films will be discussed in a subsequent publication.) This can be explained by a B-type structure. Here, the thickness of the region of parallel lamellae near the free surface is still restricted to commensurate values, but the height of the vertical lamellae is unconstrained and can take on any value. Any incommensurability is relieved by the vertical lamellae, and consequently, no surface topography forms.

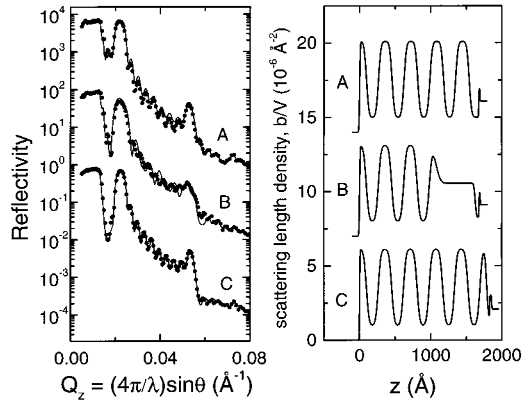

Figure 3. (a) Neutron reflectivity profiles for samples on $f = 0.0$, 0.58, and 1.0 brushes. The points are data; the lines were calculated from the fitted scattering length density profiles shown in (b). Note the suppression of the first- and third-order Bragg peaks for $f = 0.58$.

Neutron reflectivity data were taken on the NG7 reflectometer at NIST in Gaithersburg, MD, using a wavelength of $\lambda = 4.75$ Å and a resolution of $\Delta Q_z/Q_z = 5\%$, where $Q_z = (4\pi/\lambda)\sin\theta$ and θ is the grazing angle of incidence. The reflectivity was measured for a series of 11 films of nearly identical thicknesses ($t \approx 1800$ Å) on substrates with $0 \leq f \leq 1$. Just as for the optical microscopy results, the samples could be divided into three categories based on the reflectivity data. Figure 3a shows the reflectivity profiles for samples on brushes with $f = 0$, $f = 0.58$, and $f = 1$ (top to bottom), each of which is representative of the data for the other samples in their respective groups. Groups A and C show very strong, well-defined, first- and third-order Bragg peaks, with a maximum reflectivity near unity for the first-order peak. The reflectivities of groups A and C differ strongly in the Q_z region between the critical edge and the first-order peak. The solid lines are the best fit to

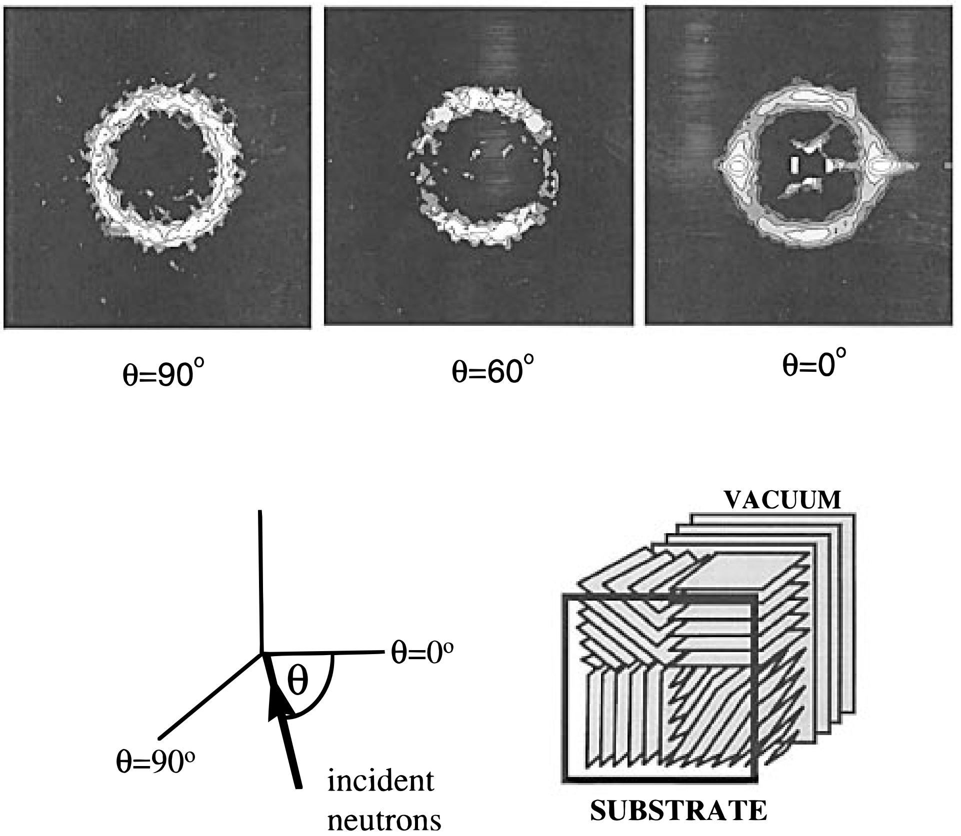

Figure 4. Small angle scattering data (after background subtraction) for a type B sample, for incidence angles of (a) 90°, (b) 60°, and (c) 0°. The scattering patterns can be understood with the help of the schematic model shown in (d).

the reflectivity profiles, calculated from the scattering length density profiles shown in Figure 3B. The reflectivity data for groups A and C are well described using a simple alternating layered morphology,[13] and the differences in the reflectivities are due to the fact that the layers adjacent to the brush are PMMA and dPS for groups A and C, respectively.

The reflectivity profiles from group B samples also exhibited a well-defined first-order peak, but the maximum intensity was reduced by ~30% compared to the reflectivity from samples in groups A and C. In addition, both the Kiessig fringes characteristic of the film thickness and the third-order Bragg peak are suppressed in the type B films. This indicates some orientation of the lamellae parallel to the films surface, but it is somehow weaker than that seen for groups A and C. The maximum reflectivities in the total reflection region, just below the critical edge at $Q_z = 0.013$, are 0.7, 0.9, and 0.75 for the group A, B, and C samples, respectively. The reduced reflectivities in the group A and C samples are due to the increased surface roughness associated with islands and holes on the surface, which results in stronger off-specular scattering. A reasonable fit to the reflectivity data of type B samples could be obtained using a model that included parallel layers near the free surface and perpendicular layers near the substrate (Figure 3b). The perpendicular layers adjacent to the substrate appear in the model as a region of uniform scattering length density, equal to the average scattering length density of the dPS and PMMA blocks.

The film thickness for the group B samples was determined ellipsometrically, and a period of $L_0 = 360$ Å, determined from fits to the group A and C reflectivity data, was used for the parallel layers. Thus, the only significant parameter varied was the *number* of layers parallel to the free surface, which fixed the thickness of the layer with constant scattering length density adjacent to the substrate. As the number of parallel lamellae is reduced, the peak intensities of the Bragg reflections decrease. By optimizing the match between the measured and calculated peak intensities, the thicknesses of the parallel and perpendicular regions are estimated as $\sim 3L_0$ (1100 Å) and $\sim 2L_0$ (700 Å) for this total film thickness. Finer details of the reflectivity data (e.g., the Kiessig fringes) are not reproduced by this crude model, but the model does capture the reduced peak intensities and the peak shapes quite well. The major deficiency of the model is likely to be its oversimplified picture of the interface between the regions of parallel and perpendicular lamellae, which may not be as simple and laterally uniform as depicted in Figure 1b.

Small angle neutron scattering (SANS) measurements provided strong complementary evidence to support the above picture. SANS data were taken on the NG3 beamline at NIST, using neutrons with a wavelength of 5 Å and a sample aperture diameter of 1.27 cm. The background from a bare substrate was subtracted from each measurement. With the neutron beam incident perpendicular to the substrate ($\theta = 90°$, where $\theta =$ is the grazing angle of incidence, defined in the same way as for the reflectivity experiments), all samples from group B yielded isotropic scattering patterns with a peak at $Q = 0.017$ Å^{-1} (Figure 4a), corresponding well to the lamellar spacing of 360 Å determined by reflectivity. None of the samples in groups A and C showed any scattering above the background in this geometry. Data were also taken on type B samples as the sample was rotated in the neutron beam. This places a component of the scattering vector normal to the plane of the film. As the sample normal is rotated away from the direction of the neutron beam, the scattering profile becomes progressively more arced (e.g., Figure 4b, for $\theta = 60°$). When the sample surface is parallel to the neutron beam, a scattering pattern is observed with intensity maxima on both the equator and meridion (Figure 4c). The strong equatorial scattering arises from the lamellae oriented parallel to the free surface. The meridional reflections are due to the lamellae oriented normal to the substrate interface. The intensities of the meridional reflections are much lower than for the equatorial reflections, since only a fraction of the lamellae are properly oriented to satisfy the Bragg condition for diffraction.

In summary, evidence from optical microscopy, neutron reflectivity, and small angle neutron scattering strongly suggests the occurrence of a “mixed” structure (both parallel and perpendicular lamellae) in unconfined block copolymer films on nearly neutral substrates. While the presence of a nearly neutral (nonpreferential) surface is clearly necessary for this structure to occur, it is not clear, at present, whether this is sufficient. Commensurability effects and the kinetics of the ordering process may also play an important role. These are currently being investigated. It is noteworthy, however, that the total SANS intensity from the group B samples is strongly dependent on the film thickness and varies in a periodic manner with film thickness.

Acknowledgment. We thank Drs. Sushil K. Satija and Li Pin Sung for assistance with neutron reflectivity measurements and Dr. Tania Slawecki for assistance with small angle neutron scattering measurements. This work was partially supported by the Department of Energy, Office of Basics Energy Sciences, the NSF Center for Polymer Interfaces and Macromolecular Assemblies (Standford/IBM/UC Davis), and the Materials Research Science and Engineering Center at the University of Massachusetts.

References and Notes

(1) Meier, D. J. *J. Polym. Sci., Part C* **1969**, *26*, 81.
(2) Helfand, E.; Wasserman, Z. R. *Macromolecules* **1976**, *9*, 879.
(3) Bates, F. S.; Fredrickson, G. H. *Annu. Rev. Phys. Chem.* **1990**, *41*, 525.
(4) Coulon, G.; Deline, V. R.; Green, P. F.; Russell, T. P. *Macromolecules* **1989**, *22*, 2581.
(5) Anastasiadis, S. H.; Russell, T. P.; Satija, S. K.; Majkrzak, C. F. *Phys. Rev. Lett.* **1989**, *62*, 1852.
(6) Henkee, C. S.; Thomas, E. L.; Fetters, L. J. *J. Mater. Sci.* **1988**, *23*, 1685.
(7) Lambooy, P.; Russell, T. P.; Kellogg, G. J.; Mayes, A. M.; Gallagher, P. D.; Satija, S. K. *Phys. Rev. Lett.* **1994**, *72* (18), 2899.
(8) Koneripalli, N.; Singh, N.; Levicky, R.; Bates, F. S.; Gallagher, P. D.; Satija, S. K. *Macromolecules* **1995**, *28*, 2897.
(9) Walton, D. G.; Kellogg, G. J.; Mayes, A. M.; Lambooy, P.; Russell, T. P. *Macromolecules* **1994**, *27*, 6225.
(10) Kellogg, G. J.; Walton, D. G.; Mayes, A. M.; Lambooy, P.; Russell, T. P.; Gallagher, P. D.; Satija, S. K. *Phys. Rev. Lett.* **1996**, *76*, 2503.
(11) Mansky, P.; Liu, Y.; Huang, E.; Russell, T. P.; Hawker, C. *Science* **1997**, *275*, 1458.
(12) Mansky, P.; Russell, T. P.; Hawker, C.; Mayes, J.; Cook, D. C.; Satija, S. K. *Phys. Rev. Lett.*, submitted for publication.
(13) Russell, T. P. *Mater. Sci. Rep.* **1990**, *5*, 171.

MA970675V